

**DEVELOPMENT AND ANALYSIS OF HYDROTALCITE-
MODIFIED POROUS MEMBRANES FOR CARBON DIOXIDE
SEPARATION**

AHMED DAHAM WIHEEB

UNIVERSITI SAINS MALAYSIA

2013

**DEVELOPMENT AND ANALYSIS OF HYDROTALCITE-
MODIFIED POROUS MEMBRANES FOR CARBON DIOXIDE
SEPARATION**

by

AHMED DAHAM WIHEEB

**Thesis submitted in fulfillment of the
requirements for the degree of
Doctor of Philosophy**

September 2013

ACKNOWLEDGMENTS

First, I would like to thank the Almighty God for his infinite mercy and protection upon the accomplishment of my studies. It is my great pleasure to express my sincere gratitude to my supervisor Assoc. Prof. Dr. Mohd Roslee Othman for his scientific and moral support, encouragement and guidance throughout this research. I thank him a lot for his invaluable ideas and remarks which made this study very interesting. I would also like to extend my heartfelt thanks to Assoc. Prof. Dr. Mohd Azmier Ahmad and Dr. Mohd Nazri Murat for their support throughout the work. I really was honored to have the opportunity to work under the supervision of all of them.

I would also like to express my appreciation to the Dean, Prof. Dr. Azlina BT. Harun @ Kamaruddin, Prof. Dr. Abdul Latif Ahmad, Assoc. Prof. Dr. Mohamad Zailani Bin Abu Bakar and Assoc. Prof. Dr. Ahmad Zuhairi Abdullah, Deputy Deans of the School of Chemical Engineering USM, for their continuous support and help rendered throughout my studies. My sincere thanks go to all the respective lecturers, staff and technicians in the School of Chemical Engineering, USM, for their cooperation and support without any hesitation.

I wish to express my acknowledgement to Membrane Science & Technology Research Cluster for supporting this research work. The fundings provided by USM under Membrane cluster (Account No.:100/PSF/81610013) and RU-PRGS (Account No.:1001/PJKIMIA/8045028) for conducting the research work are gratefully acknowledged.

I would like to extend my sincere and deepest gratitude to all my adored friends, in Malaysia and in Iraq for their unparalleled help, kindness and moral support towards me. Thank you for always being there for me. I hope we all have a very bright future undertaking ahead. Very special thanks go to my dear friends Harith, Muataz, Ali Sabri, Saad Raheem, Arkan and Abdullah, for their useful help and companionship. Also I do wish to express my deepest appreciation to Universiti Sains Malaysia for providing me a warm environment to feel at home.

Last but definitely not least, my deepest and most heartfelt gratitude to my beloved mom, for her endless love and support. I need to thank very especially to my darling wife and sweetheart sons, for all those innumerable things I could not possibly have done without them. My enormous gratitude to my parents, dear brothers and wonderful sisters for their support and encourage. To whom are directly and indirectly involved in this research, your contribution given shall not be forgotten. My appreciation goes to all of you.

Ahmed Daham Wiheeb

September 2013

TABLE OF CONTENTS

	Page
ACKNOWLEDGEMENTS	ii
TABLE OF CONTENTS	iv
LIST OF TABLES	x
LIST OF FIGURES	xiii
LIST OF PLATES	xxiii
LIST OF SYMBOLS	xxiv
LIST OF ABBREVIATION	xxvi
ABSTRAK	xxix
ABSTRACT	xxx
CHAPTER 1 - INTRODUCTION	1
1.1 Global issues of carbon dioxide as greenhouse gas	1
1.2 Conventional technologies for CO ₂ separation and capture	3
1.3 Membrane technology for CO ₂ separation	5
1.4 Hydrotalcite compound for CO ₂ separation	8
1.5 Problem Statement	10
1.6 Research objectives	12
1.7 Research scope	13
1.7.1 Synthesis of unmodified alumina and silica membranes via sol-gel method	14
1.7.2 Development of alumina and silica membranes with HT material via sol-gel method	14
1.7.3 Characterization of unmodified and the modified porous membranes	15
1.7.4 Study of the permeation of single gas and mixed gas mixtures using modified HT porous membrane	16
1.7.5 Modeling, optimization for CO ₂ permeance and separation selectivity from mixed gas mixture and surface affinity study	16

1.7	Organization of the thesis	17
CHAPTER 2 - LITERATURE REVIEW		19
2.1	γ -alumina membranes for gas separation	19
2.1.1	Synthesis of γ -alumina membrane by sol-gel method	22
2.2	Silica membranes for gas separation	24
2.2.1	Silica membranes synthesized by sol-gel method	26
2.2.2	Silica membranes synthesized by chemical vapor deposition (CVD)	32
2.2.3	Modification of silica membrane	36
2.3	Hydrotalcite compound for CO ₂ adsorption	40
2.3.1	Methods of hydrotalcite compound synthesis	42
2.3.1.a	Sol-gel method	43
2.3.2	Hydrotalcite membrane	46
2.4	Gas transport mechanisms for inorganic membranes	49
2.4.1	Viscous flow	49
2.4.2	Knudsen diffusion	50
2.4.3	Surface adsorption	51
2.4.4	Permeability accounting for all the transport mechanisms	53
CHAPTER 3 - MATERIALS AND METHODS		55
3.1	Materials and chemicals	55
3.2	Equipment	56
3.3	Preparation of membranes	58
3.3.1	Preparation of membrane support	59
3.3.2	Preparation of alumina membrane	60
3.3.3	Preparation of hydrotalcite sol	62
3.3.4	Preparation of HT-alumina composite membrane	65
3.3.5	Preparation of silica membrane	65
3.3.6	Preparation of HT-silica composite membrane	68
3.4	Characterization of the prepared membrane	69
3.4.1	Structure and phases present	70
3.4.2	Surface chemistry	70

3.4.3	Thermal stability	71
3.4.4	Textural properties	71
3.4.5	CO ₂ adsorption/desorption measurements	72
3.4.6	Surface morphology and qualification of elemental composition	73
3.5	Gas permeation and separation studies	74
3.5.1	Membrane test rig setup	74
3.5.2	Membrane permeation cell	77
3.5.3	Operation of gas permeation and separation test rig	78
3.5.3.a	Leak checking	78
3.5.3.b	Membrane pretreated and system vacuumed	79
3.5.3.c	Single gas permeation experiment	79
3.5.3.d	Mixed gas permeation and separation experiment	79
3.5.4	Gas analysis	79
3.5.5	Gas permeation durability test	80
3.5.6	Membrane performance	80
3.6	Design of experiments (DoE)	83
CHAPTER 4 – RESULTES AND DISCUSION		85
4.1	Characterization of membranes	86
4.1.1	HT-alumina membranes	86
4.1.1.a	Structure and phases present	86
4.1.1.b	Surface chemistry	87
4.1.1.c	Textural properties	88
4.1.1.d	CO ₂ adsorption/desorption measurements	90
4.4.1.e	Surface morphology	92
4.1.2	HT-silica membranes	93
4.1.2.a	Structure and phases present	93
4.1.2.b	Surface chemistry	95
4.1.2.c	Thermal stability	98
4.1.2.d	Textural properties	101
4.1.2.e	CO ₂ adsorption/desorption measurements	108
4.1.2.f	Surface morphology and qualification of elemental composition	113

4.1.3	Pore size distribution for intermediate layer and support	119
4.2	Preliminary studies for gas permeation test	121
4.2.1	Reproducibility studies of macroporous α -alumina support	121
4.2.2	Reproducibility studies of mesoporous γ -alumina membrane	124
4.2.3	Comparison of gas permeation performance for HT-alumina membranes	129
4.2.4	HT-silica membranes	130
4.2.4.a	Comparison of gas permeation performance for the composite membrane with different HT vol. %	130
4.2.4.b	Comparison of gas permeation performance for the composite membrane sintered at different temperature	134
4.3	Gas permeation and separation performance studies over S-15HT-5 membrane	138
4.3.1	Single gas permeation studies	138
4.3.2	Mixed-gas separation studies over S-15HT-5 membrane	148
4.3.2.a	Separation of CO ₂ /CH ₄ mixture	148
4.3.2.a (i)	Effect of pressure difference	148
4.3.2.a (ii)	Effect of temperature	152
4.3.2.a (iii)	Effect of CO ₂ feed concentration	155
4.3.2.b	Separation of CO ₂ /N ₂ mixture	159
4.3.2.b (i)	Effect of pressure difference	159
4.3.2.b (ii)	Effect of temperature	163
4.3.2.b (iii)	Effect of CO ₂ feed concentration	166
4.3.2.c	Separation of CO ₂ /H ₂ mixture	169
4.3.2.c (i)	Effect of pressure difference	169
4.3.2.c (ii)	Effect of temperature	174
4.3.2.c (iii)	Effect of CO ₂ feed concentration	177
4.3.3	Gas permeation durability test of S-15HT-5 membrane	180
4.4	Statistical analysis and model development using design of experiment (DoE)	182

4.4.1	Permeation and separation of CO ₂ /CH ₄ binary gas mixture	182
4.4.1.a	Full fractal design	182
4.4.1.b	Response surface modeling of CO ₂ permeance in CO ₂ /CH ₄ mixture	183
4.4.1.c	Response surface modeling of CO ₂ /CH ₄ separation selectivity	188
4.4.1.d	Process optimization using response surface methodology (RSM)	193
4.4.2	Permeation and separation of CO ₂ /N ₂ binary gas mixture	196
4.4.2.a	Full fractal design	196
4.4.2.b	Response surface modeling of CO ₂ permeance in CO ₂ / N ₂ mixture	202
4.4.2.c	Response surface modeling of CO ₂ /N ₂ separation selectivity	202
4.4.2.d	Process optimization using response surface methodology (RSM)	207
4.4.3	Permeation and separation of CO ₂ /H ₂ binary gas mixture	209
4.4.3.a	Full fractal design	209
4.4.3.b	Response surface modeling of CO ₂ permeance in CO ₂ / H ₂ mixture	210
4.4.3.c	Response surface modeling of CO ₂ /H ₂ separation selectivity	215
4.4.3.d	Process optimization using response surface methodology (RSM)	219
CHAPTER 5 – CONCLUSIONS AND RECOMMENDATIONS		222
5.1	Conclusions	222
5.2	Recommendations	225
REFERENCES		226
APPENDICES		244
Appendix A		244
A.1	Photographs of prepared sols	244
A.2	Photographs of HT sol preparation apparatus	245

	A.3	Photographs of membrane test rig	246
Appendix B			248
	B.1	Leak checking procedure	248
	B.2	Membrane pretreated and system vacuumed	248
	B.3	Single gas permeation experiment procedure	249
	B.4	Mixed gas permeation and separation experiment procedure	250
Appendix C			252
	C.1	GC analysis for CO ₂ , H ₂ , N ₂ , CH ₄ , CO ₂ /CH ₄ , CO ₂ /N ₂ and CO ₂ /H ₂ gases	252
	C.2	GC Standard Curve for CO ₂ , H ₂ , N ₂ and CH ₄ gases	254
Appendix D			255
	D.1	Membrane performance analysis for the single gas permeations through S-15HT-5 membrane	255
	D.2	Membrane performance analysis for the mixed gas permeations and separations through S-15HT-5 membrane	257
LIST OF PUBLICATIONS			263

LIST OF TABLES

		Page
Table 2.1	Summary of reported CO ₂ gas permeation and separation results from different silica membranes prepared by sol-gel method	31
Table 2.2	Summary of reported CO ₂ gas permeation and separation results from different tubular silica membranes prepared by CVD method	35
Table 2.3	Summary of reported CO ₂ gas permeation and separation results from different metal-silica membranes	38
Table 2.4	Molecular weight and kinetic diameter of various gases encountered in membrane gas separation	54
Table 3.1	List of chemicals used for this research	56
Table 3.2	List of equipment and facilities used through this research	57
Table 3.3	Coded label of the HT-silica composite membranes synthesized in this study	69
Table 4.1	Summarized isothermal adsorption result of HT-alumina samples containing different HT vol. %, at 30 °C	91
Table 4.2	Summarized TGA weight loss for powder samples	101
Table 4.3	Summarized isothermal adsorption result for sorbents at 30 °C	110
Table 4.4	Single gas flow rate for different gases through α -alumina support at 100 kPa pressure difference and 30 °C	121
Table 4.5	Permeances and permselectivities for different gases through α -alumina support at 100 kPa pressure difference and 30 °C	123
Table 4.6	Weight gained by the two coated γ -alumina layers on α -alumina support	125
Table 4.7	Single gas permeation through mesoporous γ -alumina membrane coated on α -alumina support at 100 kPa pressure difference and 30 °C	125

Table 4.8	Permeances and permselectivities for different gases through mesoporous γ -alumina membrane coated on α -alumina support at 100 kPa pressure difference and 30 °C	127
Table 4.9	Permeate flow studies at 100 kPa pressure difference and 30 °C for different ratio of HT in composite membrane sintered at 500 °C	131
Table 4.10	Permeate flow studies through S-15HT-5 membrane at 100 kPa pressure difference and 30 °C for different sintering temperatures	135
Table 4.11	Experiment matrix and responses for the permeation and separation of CO ₂ /CH ₄ gas mixture using S-15HT-5 membrane	183
Table 4.12	ANOVA results for CO ₂ permeance in the CO ₂ /CH ₄ binary mixture	184
Table 4.13	ANOVA results for separation selectivity in the CO ₂ /CH ₄ gas mixture	189
Table 4.14	Constraint used for optimization of CO ₂ permeance and separation selectivity of the CO ₂ /CH ₄ binary gas mixture	194
Table 4.15	Optimum condition of CO ₂ permeance and separation selectivity of the CO ₂ /CH ₄ binary gas mixture	195
Table 4.16	Experiments at optimum conditions simulated by DoE for the CO ₂ permeance and separation selectivity of CO ₂ /CH ₄ binary gas mixture	196
Table 4.17	Experiment matrix and responses for the permeation and separation of CO ₂ /N ₂ binary gas mixture using S-15HT-5 membrane	197
Table 4.18	ANOVA results for CO ₂ permeance of the CO ₂ /N ₂ binary mixture	198
Table 4.19	ANOVA results for separation selectivity of the CO ₂ /N ₂ binary gas mixture	203
Table 4.20	Constraint used for optimization of CO ₂ permeance and separation selectivity of the CO ₂ /N ₂ binary gas mixture	207

Table 4.21	Optimum condition of CO ₂ permeance and separation selectivity of the CO ₂ /N ₂ binary gas mixture	208
Table 4.22	Verification experiments at optimum conditions simulated by DoE for the CO ₂ permeance and separation selectivity of the CO ₂ /N ₂ binary gas mixture	209
Table 4.23	Experiment matrix and responses for the permeation and separation of CO ₂ /H ₂ binary gas mixture using S-15HT-5 membrane	210
Table 4.24	ANOVA results for CO ₂ permeance of the CO ₂ /H ₂ binary gas mixture	211
Table 4.25	ANOVA results for separation selectivity of the CO ₂ /H ₂ binary gas mixture	215
Table 4.26	Constraint used for optimization of CO ₂ permeance and separation selectivity of the CO ₂ /H ₂ binary gas mixture	219
Table 4.27	Optimum condition of CO ₂ permeance and separation selectivity of the CO ₂ /H ₂ binary gas mixture	220
Table 4.28	Verification experiments at optimum conditions simulated by DoE for the CO ₂ permeance and separation selectivity of the CO ₂ /H ₂ binary gas mixture	221
Table D.1.1	Raw data for gas permeation measurement using bubble flowmeter	255
Table D.1.2	Calculated mole flux and permeance of all used gases	256
Table D.2.1	Total gas flow rate and CO ₂ compositions for CO ₂ /CH ₄ mixed gas at different streams	259

LIST OF FIGURES

		Page
Figure 1.1	Schematic representation of the HT structure	10
Figure 2.1	Schematic diagram of silicon alkoxide hydrolysis in acid and basic conditions	27
Figure 2.2	Schematic diagram of condensation reaction and mechanism under acid and basic conditions	29
Figure 2.3	Schematic diagram of a typical CVD process	33
Figure 2.4	The thermal evolution of hydrotalcite as a function of temperature	41
Figure 2.5	The structure of brucite	42
Figure 3.1	The schematic diagram of the experiment	58
Figure 3.2	Sintering temperature profile for α -alumina support	59
Figure 3.3	Sintering temperature profile for γ - Al_2O_3 membrane	61
Figure 3.4	Flow chart for preparation of γ - Al_2O_3 membrane by sol-gel method	62
Figure 3.5	Schematic diagram of HT sol preparation setup	63
Figure 3.6	Flow chart for preparation of HT sol	64
Figure 3.7	Sintering temperature profile for silica membrane	67
Figure 3.8	Flow chart for preparation of silica membrane by sol-gel method	68
Figure 3.9	Schematic diagram of membrane test rig	75
Figure 3.10	Schematic diagram of membrane permeation cell	78
Figure 4.1	XRD patterns of the HT-alumina samples containing different HT vol. %: (a) 0% (pure alumina); (b) 3 % and (c) 6 %, sintered at 500 °C	86

Figure 4.2	FT-IR spectra of HT-alumina samples containing different HT vol. %: (a) 0% (pure alumina); (b) 3 % and (c) 6 %, sintered at 500 °C	88
Figure 4.3	Nitrogen adsorption–desorption isotherms of HT-alumina samples containing different HT vol. %: (a) 0% (pure alumina); (b) 3 % and (c) 6 % and (d) 100 % HT, sintered at 500 °C	89
Figure 4.4	Pore size distribution of HT-alumina samples containing different HT vol. %	90
Figure 4.5	Isothermal adsorption-desorption of HT-alumina samples containing different HT vol. %, at 30 °C	91
Figure 4.6	SEM images of HT-alumina membrane containing 6 vol. % HT: (a) surface measures at 50 μm, (c) surface measures at 5 μm (c) cross sectional view measures at 100 μm and (d) cross sectional view measures at 30 μm	92
Figure 4.7	XRD patterns of the unsupported membranes: (a) S-5; (b) S-10HT-5; (c) S-15HT-5; (d) S-20HT-5; (e) S-25HT-5 and (f) HT-5, sintered at 500 °C	94
Figure 4.8	XRD patterns of the unsupported HT-silica composite membranes sintered at different temperature: (a) 400 °C; (b) 500 °C; (c) 600 °C and (d) 700 °C	95
Figure 4.9	FT-IR spectra of unsupported membranes with different HT ratios: (a) S-5; (b) S-10HT-5; (c) S-15HT-5; (d) S-20HT-5 and (e) S-25HT-5, sintered at 500 °C	97
Figure 4.10	FT-IR spectra of unsupported S-15HT-5 composite membrane: (a) before and (b) after sintered at 500 °C	98
Figure 4.11	TGA-DTG profile of (a) S-5; (b) S-10HT-5; (c) S-15HT-5; (d) S-20HT-5 and (e) S-25HT-5 powder samples	99
Figure 4.12	Nitrogen adsorption–desorption isotherms for silica as well as for HT-silica composite membranes sintered at 500 °C for 3 h	102
Figure 4.13	Effect of HT vol. % on total pore volume and micropore percentage for silica and composite membranes sintered at 500 °C for 3 h	103

Figure 4.14	Effect of HT ratio on BTE surface area and pore width for silica and composite membranes sintered at 500 °C for 3 h	104
Figure 4.15	Effect of sintering temperature on total pore volume and micropore percentage for composite membrane with 15 vol. % of HT	105
Figure 4.16	Effect of sintering temperature on BTE surface area and pore width for composite membrane with 15 vol. % of HT	107
Figure 4.17	Pore size distribution of S-5 and S-15HT-5 unsupported material by the Horváth-Kawazoe method	108
Figure 4.18	Isothermal adsorption-desorption of silica and HT-silica membranes at 30 °C	109
Figure 4.19	Three cycles of isothermal adsorption-desorption for S-15HT-5	111
Figure 4.20	CO ₂ adsorption capacity of three cycles at 30 °C for composite membranes with different HT vol. % sintered at 500 °C	112
Figure 4.21	CO ₂ adsorption capacity of three cycles at 30°C for S-15HT-5 composite membranes sintering at different temperatures	113
Figure 4.22	SEM images (a) α -alumina support, (b) γ -alumina, (c) S-5 and (d) S-15HT-5 top surfaces	115
Figure 4.23	SEM images of membranes cross sectional view of (a) intermediate layer of γ -alumina, (b) S-5 measures at 5 μ m, (c) S-5 measures at 2 μ m, (d) S-15HT-5 measures at 5 μ m and (e) S-15HT-5 measures at 2 μ m	116
Figure 4.24	EDX analysis of (a) γ -alumina, (b) S-5 and (c) S-15HT-5 membranes	118
Figure 4.25	Pore size distribution of (a) macro-porous α -alumina support and (b) meso-porous γ -alumina layer sintered at 600 °C	120
Figure 4.26	Permeances of pure gases across α -alumina support at 30 °C	124

Figure 4.27	Permeances of pure gases across γ -alumina membrane at 30 °C	128
Figure 4.28	Permeances of pure gases across γ -alumina at 100 kPa pressure difference and 30 °C are dependent on molecular weight	128
Figure 4.29	Permselectivities of CO ₂ /H ₂ , CO ₂ /N ₂ , CO ₂ /CH ₄ and CO ₂ permeance at 100 kPa pressure difference and 30 °C for HT-alumina composite membranes containing different HT vol. % sintered at 500 °C	130
Figure 4.30	Single gas permeances of CO ₂ , H ₂ , N ₂ and CH ₄ at 100 kPa pressure difference and 30 °C for different vol. % of HT in composite membrane sintered at 500 °C	133
Figure 4.31	Permselectivities of CO ₂ /H ₂ , CO ₂ /N ₂ and CO ₂ /CH ₄ at 100 kPa pressure difference and 30 °C for different vol. % of HT in composite membrane sintered at 500 °C	134
Figure 4.32	Single gas permeances of CO ₂ , H ₂ , N ₂ and CH ₄ through S-15HT-5 membrane at 100 kPa pressure difference and 30 °C for different sintering temperatures	136
Figure 4.33	Permselectivities of CO ₂ /H ₂ , CO ₂ /N ₂ and CO ₂ /CH ₄ through S-15HT-5 membrane at 100 kPa pressure difference and 30 °C for different sintering temperatures	137
Figure 4.34	Permeate fluxes of (a) CO ₂ , (b) H ₂ , (c) N ₂ and (d) CH ₄ single gases across S-15HT-5 membrane as a function of pressure difference at (30-90 °C) temperature range	139
Figure 4.35	Single gas permeances through S-15HT-5 membrane at 30 °C as a function of pressure difference across the membrane	142
Figure 4.36	Single gas permeances through S-15HT-5 membrane at 100 kPa pressure difference across the membrane as a function of temperature	144
Figure 4.37	CO ₂ permeance through S-15HT-5 membrane as a function of pressure difference across the membrane at (30-190 °C) temperature range	145

Figure 4.38	Permselectivities of (a) CO ₂ /CH ₄ , (b) CO ₂ /N ₂ and (c) CO ₂ /H ₂ through S-15HT-5 membrane as a function of pressure difference across the membrane at (30-190 °C) temperature range	146
Figure 4.39	Permeate fluxes of CO ₂ and CH ₄ gases and CO ₂ /CH ₄ flux ratio through S-15HT-5 membrane for a CO ₂ /CH ₄ mixture (50/50 feed) at 30 °C as a function of pressure difference across the membrane	149
Figure 4.40	CO ₂ and CH ₄ permeances through S-15HT-5 membrane for a CO ₂ /CH ₄ mixture (50/50 feed) at 30 °C as a function of pressure difference across the membrane	150
Figure 4.41	Separation selectivity and selectivity through S-15HT-5 membrane for a CO ₂ /CH ₄ mixture (50/50 feed) at 30 °C as a function of pressure difference across the membrane	152
Figure 4.42	Permeate fluxes of CO ₂ and CH ₄ gases and CO ₂ /CH ₄ flux ratio through S-15HT-5 membrane for a CO ₂ /CH ₄ mixture (50/50 feed) at 100 kPa pressure difference across the membrane as a function of temperature	153
Figure 4.43	CO ₂ and CH ₄ permeances through S-15HT-5 membrane for a CO ₂ /CH ₄ mixture (50/50 feed) at 100 kPa pressure difference across the membrane as a function of temperature	154
Figure 4.44	Separation selectivity and selectivity through S-15HT-5 membrane for a CO ₂ /CH ₄ mixture (50/50 feed) at 100 kPa pressure difference across the membrane as a function of temperature	155
Figure 4.45	Permeate fluxes of CO ₂ and CH ₄ gases and CO ₂ /CH ₄ flux ratio through S-15HT-5 membrane for a CO ₂ /CH ₄ mixture as a function of CO ₂ feed concentration at 100 kPa pressure difference across the membrane and 30 °C temperature	156
Figure 4.46	CO ₂ and CH ₄ permeances through S-15HT-5 membrane for a CO ₂ /CH ₄ mixture as a function of CO ₂ feed concentration at 100 kPa pressure difference across the membrane and 30 °C temperature	157

Figure 4.47	Separation selectivity and selectivity through S-15HT-5 membrane for a CO ₂ /CH ₄ mixture as a function of CO ₂ feed concentration at 100 kPa pressure difference across the membrane and 30 °C temperature	158
Figure 4.48	Permeate fluxes of CO ₂ and N ₂ gases and CO ₂ /N ₂ flux ratio through S-15HT-5 membrane for a CO ₂ /N ₂ mixture (50/50 feed) at 30 °C as a function of pressure difference across the membrane	160
Figure 4.49	CO ₂ and N ₂ permeances through S-15HT-5 membrane for a CO ₂ /N ₂ mixture (50/50 feed) at 30 °C as a function of pressure difference across the membrane	161
Figure 4.50	Separation selectivity and selectivity through S-15HT-5 membrane for a CO ₂ /N ₂ mixture (50/50 feed) at 30 °C as a function of pressure difference across the membrane	163
Figure 4.51	Permeate fluxes of CO ₂ and N ₂ gases and (CO ₂ /N ₂) flux Ratio through S-15HT-5 membrane for a CO ₂ /N ₂ mixture (50/50 feed) at 100 kPa pressure difference across the membrane as a function of Temperature	164
Figure 4.52	CO ₂ and N ₂ permeances through S-15HT-5 membrane for a CO ₂ /N ₂ mixture (50/50 feed) at 100 kPa pressure difference across the membrane as a function of temperature	165
Figure 4.53	Separation selectivity and selectivity through S-15HT-5 membrane for a CO ₂ /N ₂ mixture (50/50 feed) at 100 kPa pressure difference across the membrane as a function of temperature	166
Figure 4.54	Permeate fluxes of CO ₂ and N ₂ gases and CO ₂ /N ₂ flux ratio through S-15HT-5 membrane for a CO ₂ /N ₂ mixture as a function of CO ₂ feed concentration at 100 kPa pressure difference across the membrane and 30 °C temperature	167
Figure 4.55	CO ₂ and N ₂ permeances through S-15HT-5 membrane for a CO ₂ /N ₂ mixture as a function of CO ₂ feed concentration at 100 kPa pressure difference across the membrane and 30 °C temperature	168

Figure 4.56	Separation selectivity and selectivity through S-15HT-5 membrane for a CO ₂ /N ₂ mixture as a function of CO ₂ feed concentration at 100 kPa pressure difference across the membrane and 30 °C	169
Figure 4.57	Permeate fluxes of CO ₂ and H ₂ gases and CO ₂ /H ₂ flux ratio through S-15HT-5 membrane for a CO ₂ /H ₂ mixture (50/50 feed) at 30 °C as a function of pressure difference across the membrane	171
Figure 4.58	CO ₂ and H ₂ permeances through S-15HT-5 membrane for a CO ₂ /H ₂ mixture (50/50 feed) at 30 °C as a function of pressure difference across the membrane	172
Figure 4.59	Separation selectivity and selectivity through S-15HT-5 membrane for a CO ₂ /H ₂ mixture (50/50 feed) at 30 °C as a function of pressure difference across the membrane	173
Figure 4.60	Permeate fluxes of CO ₂ and H ₂ gases and CO ₂ /H ₂ flux ratio through S-15HT-5 membrane for a CO ₂ /H ₂ mixture (50/50 feed) at 100 kPa pressure difference across the membrane as a function of temperature	175
Figure 4.61	CO ₂ and H ₂ permeances through S-15HT-5 membrane for a CO ₂ /H ₂ mixture (50/50 feed) at 100 kPa pressure difference across the membrane as a function of temperature	176
Figure 4.62	Separation selectivity and selectivity through S-15HT-5 membrane for a CO ₂ /H ₂ mixture (50/50 feed) at 100 kPa pressure difference across the membrane as a function of temperature	177
Figure 4.63	Permeate fluxes of CO ₂ and H ₂ gases and CO ₂ /H ₂ flux ratio through S-15HT-5 membrane for a CO ₂ /H ₂ mixture as a function of CO ₂ feed concentration at 100 kPa pressure difference across the membrane and 30 °C	178
Figure 4.64	CO ₂ and H ₂ permeances through S-15HT-5 membrane for a CO ₂ /H ₂ mixture as a function of CO ₂ feed concentration at 100 kPa pressure difference across the membrane and 30 °C temperature	179
Figure 4.65	Separation selectivity and selectivity through S-15HT-5 membrane for a CO ₂ /H ₂ mixture as a function of CO ₂	180

feed concentration at 100 kPa pressure difference across the membrane and 30 °C

Figure 4.66	Durability test for permeation of CO ₂ , H ₂ , N ₂ and CH ₄ gases through S-15HT-5 membrane at 100 kPa pressure difference and 30 °C	181
Figure 4.67	Effect of pressure difference across the S-15HT-5 membrane and temperature on CO ₂ permeance at 30% CO ₂ feed concentration	187
Figure 4.68	Effect of pressure difference across the S-15HT-5 membrane and CO ₂ feed concentration on CO ₂ permeance at temperature of 110 °C	187
Figure 4.69	Effect of temperature and CO ₂ feed concentration on CO ₂ permeance at pressure difference across the S-15HT-5 membrane of 300 kPa	188
Figure 4.70	Effect of pressure difference across the S-15HT-5 membrane and temperature on CO ₂ /CH ₄ separation selectivity at 30% CO ₂ feed concentration	192
Figure 4.71	Effect of pressure difference across the S-15HT-5 membrane and CO ₂ feed concentration on CO ₂ /CH ₄ separation selectivity at temperature of 110 °C	192
Figure 4.72	Effect of temperature and CO ₂ feed concentration on CO ₂ /CH ₄ separation selectivity at pressure difference across the S-15HT-5 membrane of 300 kPa	193
Figure 4.73	Effect of pressure difference across the S-15HT-5 membrane and temperature on CO ₂ permeance at 30% CO ₂ feed concentration	200
Figure 4.74	Effect of pressure difference across the S-15HT-5 membrane and CO ₂ feed concentration on CO ₂ permeance at temperature of 110 °C	201
Figure 4.75	Effect of temperature and CO ₂ feed concentration on CO ₂ permeance at pressure difference across the S-15HT-5 membrane of 300 kPa	201
Figure 4.76	Effect of pressure difference across the S-15HT-5 membrane and temperature on CO ₂ /N ₂ separation	205

selectivity at 30% CO₂ feed concentration

Figure 4.77	Effect of pressure difference across the S-15HT-5 membrane and CO ₂ feed concentration on CO ₂ /N ₂ separation selectivity at temperature of 110 °C	206
Figure 4.78	Effect of temperature and CO ₂ feed concentration on CO ₂ /N ₂ separation selectivity at pressure difference across the S-15HT-5 membrane of 300 kPa	206
Figure 4.79	Effect of pressure difference across the S-15HT-5 membrane and temperature on CO ₂ permeance at 30% CO ₂ feed concentration	213
Figure 4.80	Effect of pressure difference across the S-15HT-5 membrane and CO ₂ feed concentration on CO ₂ permeance at temperature of 110 °C	214
Figure 4.81	Effect of temperature and CO ₂ feed concentration on CO ₂ permeance at pressure difference across the S-15HT-5 membrane of 300 kPa	214
Figure 4.82	Effect of pressure difference across the S-15HT-5 membrane and temperature on CO ₂ /H ₂ separation selectivity at 30% CO ₂ feed concentration	217
Figure 4.83	Effect of pressure difference across the S-15HT-5 membrane and CO ₂ feed concentration on CO ₂ /H ₂ separation selectivity at temperature of 110 °C	218
Figure 4.84	Effect of temperature and CO ₂ feed concentration on CO ₂ /H ₂ separation selectivity at pressure difference across the S-15HT-5 membrane of 300 kPa	219
Figure C.1.1	Chromatogram of (a) CO ₂ , (b) H ₂ , (c) N ₂ , (d) CH ₄ , (e) CO ₂ /CH ₄ binary gas mixture of 60% CO ₂ , (f) CO ₂ /N ₂ binary gas mixture of 60% CO ₂ and (g) CO ₂ /H ₂ binary gas mixture of 60% CO ₂	252
Figure C.2.1	Standard Curve for (a) CO ₂ , (b) H ₂ , (c) N ₂ and (d) CH ₄	254
Figure D.2.1	Chromatogram of CO ₂ /CH ₄ binary gas mixture at (a) permeate and (b) retentate streams	257
Figure D.2.2	Chromatogram of CO ₂ /N ₂ binary gas mixture at (a) permeate and (b) retentate streams	258

Figure D.2.3 Chromatogram of CO₂/H₂ binary gas mixture at (a) 258 permeate and (b) retentate streams

LIST OF PLATES

	Page
Plate A.1.1 Photographs of prepared sols (a) Boehmite (alumina), (b) HT, (c) 6 vol. % HT-alumina, (d) silica and (e) 15 vol. % HT-silica	244
Plate A.2.1 Photographs of HT sol preparation apparatus (a) alcoholysis and partial hydrolysis step and (b) addition of magnesium methoxide step	245
Plate A.3.1 Photograph of membrane test rig (front view) with GC	246
Plate A.3.2 Photograph of membrane test rig (back view)	246
Plate A.3.3 Photograph of membrane permeation cell	247

LIST OF SYMBOLS

Symbol	Description	Unit
A	Surface area	m^2
A	Factor code of pressure difference	-
B	Factor code of temperature	-
C	Factor code of CO ₂ feed concentration	-
D_s	Surface diffusivity	cm^2/s
F	Mole flow rate	mol/s
f	Amount of adsorbed gases on the membrane surface	cm^3/g
ΔH_{ads}	Heat of adsorption	kJ/mol
K	Gas permeance	$mol/m^2.s.Pa$
L	Length of the cylindrical pore	cm
M	Molecular weight	g/gmol
N	Mole flux	$mol/m^2.s$
\bar{P}	Average feed pressure	Pa
P_H	Pressure in feed side	Pa
P_L	Pressure in permeate side	Pa
ΔP	Pressure difference	Pa
q	Volumetric flow rate	cm^3/s
R	Radius of the cylindrical pore	cm
R	Gas constant	J/mol.K
R^2	Regression coefficient	-
r_g	Gas kinetic radius	cm
r_p	Pore radius	cm
t	Actual flow path of gas molecule through the membrane	cm
T	Temperature	°C or K
t_m	Membrane thickness	cm
x	Mole fraction of gas species in the retentate stream	-

y	Mole fraction of gas species in the permeate stream	-
z	Compressibility factor	-

Greek letters

α	Selectivity	-
β	Regression coefficient	-
ε	Membrane porosity	-
μ	Gas viscosity	-
τ	Membrane tortuosity	-

Subscripts

F	Feed	-
i, j	Component gas CO ₂ , H ₂ , N ₂ or H ₂	-
m	membrane	-
p	Permeate stream	-
R	Retentate	-

Superscripts

com	composition	-
mix	Mixture	-
s	Single	-
sep	Separation selectivity	-

LIST OF ABBREVIATION

Symbol	Description
AA	Acetic acid
Al	Aluminum
Al(OC ₄ H ₉) ₃	Aluminum tri-sec-butoxide
Al(OH) ₃	Aluminum hydroxide
Al ₂ O ₃	Alumina
α-Al ₂ O ₃	Alpha alumina
γ-Al ₂ O ₃	Gamma alumina
ANOVA	Analysis of variance
Ar	Argon
ATB	Aluminum tri-sec-butoxide
BET	Brunauer-Emmett-Teller
BIH	Barret-Joyner-Halenda
BRB	Back pressure regulator
CCD	Central composite design
CMS	Carbon molecular sieve
CV	Check valve
CVD	Chemical vapor deposition
Dev	Standard Deviation
DF	Degree of Freedom
DI	Deionized
DoE	Design of experiment
DTG	Thermogravimetric Analysis

EDX	Energy dispersive X-ray
ER	Eksperimen rekabentuk
EtOH	Ethanol
FTIR	Fourier transform infrared
GC	Gas chromatography
GHG	Greenhouse gases
KBr	Potassium bromide
LDH	Layered double hydroxide
MEA	Monoethanolamine
MFC	Mass flow controller
MPR	Metodologi permukaan respon
NV	Needle valve
O ₃	Ozone
PG	Pressure gauge
“Prob>F”	Probability
PSA	Pressure swing adsorption
PVA	Polyvinyl alcohol
RSM	Response surface methodology
SEM	Scanning Electron Microscopy
SiO ₂	Silicon dioxide
TEOS	Tetraethylorthosilicate
TGA	Temperature Gravimetric Analysis
TiO ₂	Titanium dioxide
TSA	Temperature swing adsorption

TWV	Three way valve
XRD	X-ray differaction
ZrO ₂	Zirconium dioxide

PEMBANGUNAN DAN ANALISIS HIDROTALISIT-MEMBRAN-MEMBRAN BERLIANG TERUBAHSUAI UNTUK PEMISAHAN KARBON DIOKSIDA

ABSTRAK

Pembebasan karbon dioksida (CO₂) telah menjadi salah satu daripada masalah persekitaran yang paling serius semenjak revolusi perindustrian. Hari ini, pengurangan pelepasan CO₂ dianggap amat penting demi mengelak perubahan iklim global dan pemanasan global. Untuk ini, pemisahan CO₂ daripada campuran gas sedang giat dilaksanakan. Objektif utama penyelidikan ini ialah pemisahan CO₂ daripada aliran gas sintetik yang terdiri daripada campuran gas binari dengan menggunakan teknologi membran tak-organik. Penyelidikan difokuskan kepada sintesis dan pembangunan membran tak-organik berliang yang terubahsuai dengan hidrotalsit bagi membantu pemisahan CO₂. Bahan hidrotalsit telah digabung bagi memperbaiki afiniti CO₂ dan penstabilan terma membran tak-organik untuk pemisahan gas CO₂. Membran berliang meso HT-alumina (~10 µm) yang bebas daripada rekahan dan berliang mikro HT-silika (~200 nm) telah berjaya disintesis di atas lapisan γ-Al₂O₃ yang disokong oleh penyokong cakera α-Al₂O₃ menggunakan teknik sol-gel dan balut-rendam. Kesan pembolehubah ke atas prestasi membran, struktur dan kaitan ciri telapan dan mekanisma pengangkutan dipelajari dengan cara mengubah komposisi hidrotalsit dan suhu penyinteran. Membran yang tidak disokong dicari untuk mengetahui kehadiran HT, kumpulan berfungsi permukaan, topografi permukaan dan morfologi, kawasan permukaan, saiz liang, penjerapan CO₂ dan kapasiti penyah-jeupan.

Pencirian ini dilakukan dengan menggunakan kaedah penyerakan sinar-x (XRD), FTIR, SEM, EDX, BET, TGA. Pengubahsuaian membran berliang dengan

HT meningkatkan prestasi pemisahan CO₂. Membran komposit HT-silika yang mengandung 15 isipadu% HT dan disinter pada suhu 500 °C memberikan peningkatan tertinggi dalam kepilihan telapan CO₂/CH₄, CO₂/N₂ dan CO₂/H₂ masing-masing 42.65, 37.78 dan 6.34, dengan penelapan CO₂ tertinggi sebanyak $4.8 \times 10^{-7} \text{ mol.m}^{-2}.\text{s}^{-1}.\text{Pa}^{-1}$ berbanding membran HT-alumina di dalam kajian penelapan gas tulen. Membran komposit HT-silika yang mengandung 15 isipadu % HT diuji untuk kajian penyerapan gas tulen CO₂, H₂, N₂ dan CH₄ pada suhu operasi berlainan dan perbezaan tekanan. Penelapan gas campuran dan pemisahan CO₂/CH₄, CO₂/N₂ dan CO₂/H₂ juga dikaji disekitar suhu (30-190°C), perbezaan tekanan (100-500 kPa) dan kepekatan suapan CO₂ (10-50 %). Membran komposit HT-silika yang mengandung 15 isipadu % HT memberikan peningkatan tertinggi kepemilihan dalam CO₂/CH₄, CO₂/N₂ dan CO₂/H₂ masing-masing sebanyak 104.4, 68.2 and 9.3, berbanding kepilihan telapan. Eksperimen rekabentuk (ER) telah digunakan untuk mengoptimumkan dan membangunkan model empirikal bagi penelapan CO₂ kajian kepemilihan campuran gas CO₂/CH₄, CO₂/N₂ dan CO₂/H₂ pada julat suhu (30-190°C), perbezaan tekanan (100-500 kPa) dan kepekatan suapan CO₂ (10-50 %). Perisian ER dengan metodologi permukaan respon (MPR) memberikan persamaan empirikal dengan keboleh-ramalan yang baik dan keboleh-percayaan yang cukup bagi pemodelan dan ramalan prestasi membran HT-silika.

DEVELOPMENT AND ANALYSIS OF HYDROTALCITE-MODIFIED POROUS MEMBRANES FOR CARBON DIOXIDE SEPARATION

ABSTRACT

The emission of carbon dioxide (CO₂) has become one of the most serious environmental problems since the industrial revolution. Today, reducing CO₂ emissions is considered extremely important in order to abate the global climate change and global warming. For this purpose, CO₂ separations from gas mixtures have been actively researched. The main objective of this research is to separate CO₂ from the synthetically produced gas stream containing binary gas mixtures using inorganic membrane technology. The research focused on the synthesis and development of different porous inorganic membranes modified with hydrotalcite (HT) to facilitate the separation of CO₂. Hydrotalcite material was incorporated to improve the CO₂ affinity and the thermal stability of the inorganic membranes for CO₂ gas separation. The crack free mesoporous HT-alumina (~10 μm) and microporous HT-silica (~200 nm) porous membranes were successfully synthesized on top of γ-Al₂O₃ layer supported by a α-Al₂O₃ disc support using the sol-gel and dip-coating techniques. The effect of different parameters on the membrane performance, the structure and permeation properties relationships and the transport mechanism were studied by varying hydrotalcite compositions and sintering temperatures. The unsupported membranes were characterized for the presence of HT, surface functional groups, surface topography and morphology, surface area, pore size, CO₂ adsorption and desorption capacity.

These characterizations were done using X-ray diffraction (XRD), Fourier Transform Infrared (FTIR) spectrometry, scanning electron microscopy (SEM), Energy-Dispersive X-ray spectroscope, Brunauer-Emmett-Teller method (BET) and Thermo gravimetric analyzer (TGA) techniques. The modification of porous membranes with HT enhanced CO₂ separation performance. The HT-silica composite membrane containing 15 vol.% HT and sintering temperature of 500 °C gave the highest increase in CO₂/CH₄, CO₂/N₂ and CO₂/H₂ permselectivity of 42.65, 37.78 and 6.34, respectively, with the highest CO₂ permeance of 4.8×10^{-7} mol.m⁻².s⁻¹.Pa⁻¹ compared to HT-alumina membranes in preliminary pure gas permeation studies. The HT-silica composite membrane containing 15 vol.% HT was tested for pure gas permeation studies of CO₂, H₂, N₂ and CH₄ at different operating temperatures and pressure differences. The mixed gas permeation and separation of CO₂/CH₄, CO₂/N₂ and CO₂/H₂ was also studied for wide range of temperature (30-190°C), pressure difference (100-500 kPa) and CO₂ feed concentration (10-50 %). The HT-silica composite membrane containing 15 vol.% HT provided the highest increase in CO₂/CH₄, CO₂/N₂ and CO₂/H₂ separation selectivity of 104.4, 68.2 and 9.3, respectively, compared to permselectivity. The design of experiments (DoE) was used to optimize and build up an empirical model for the CO₂ permeance and separation selectivity studies of CO₂/CH₄, CO₂/N₂ and CO₂/H₂ mixed gases at wide range of temperature (30-190°C), pressure difference (100-500 kPa) and CO₂ feed concentration (10-50 %). The DoE software with response surface methodology (RSM) produced empirical equations with good predictability and sufficient reliability for the modeling and predicting the HT-silica membrane performance.

CHAPTER 1

INTRODUCTION

1.1 Global issues of carbon dioxide as greenhouse gas

Several greenhouse gases (GHG) exist in the earth's atmosphere such as carbon dioxide (CO₂), water vapor (H₂O), methane (CH₄), nitrous oxide (N₂O) and ozone (O₃) (Mondal *et al.*, 2012). These gases allow direct sunlight (relative shortwave energy) to enter the atmosphere and reach the earth's surface unimpeded. When the shortwave energy strikes the earth's surface, some of it (longer-wave (infrared) energy) is reradiated back towards the atmosphere as infrared radiation (heat). Greenhouse gases absorb this infrared radiation and trap the heat in the lower atmosphere (Carpenter *et al.*, 2013). GHG results in an increase of the average earth temperature above what it would be in the absence these gases (Rohde *et al.*, 2012). The rise in the average earth temperature may, in turn, leads to change of the weather, rising sea levels due to melting of iceberg at the pole, changes in ecosystems, loss of biodiversity and reduction of crop yield, usually referred to as "climate change" (Houghton *et al.*, 2001; Hunter *et al.*, 2013). The anthropogenic carbon dioxide has been known to cause irreversible change in ocean chemistry that could endanger marine life populations on a huge scale (Pires *et al.*, 2011; Crim *et al.*, 2011). In addition, increasing GHG concentrations affect the composition of the atmosphere and lead to the depletion of the stratospheric ozone layer.

The first measurements made in the second half of the twentieth century show that CO₂ concentration in atmosphere had increased. The concentrations of CO₂ in the atmosphere were only slightly changed before the industrial revolution

from 280 ppmv in 1000 to 295 ppmv in 1900 based on antarctica ice core data. It increased to 315 ppmv in 1958 and further to 377 ppmv in 2004 based on actual data logged in Hawaii (Yang *et al.*, 2008; Humlum *et al.*, 2013). At present, there are around 390.5 ppmv (Humlum *et al.*, 2013), an increase of over 39 percent. International Panel on Climate Change (IPCC) forecasts that, the concentration of CO₂ in the atmosphere may go up to reach 570 ppmv by the year 2100, causing a rise of average earth temperature of around 1.9°C and an increase in mean sea level of 38 cm (Stewart and Hessami, 2005). The ever increasing anthropogenic CO₂ emissions (i.e., emissions produced by human activities) since the beginning of the industrial age, has been due to the burning of huge amounts of fossil fuels, such as coal or natural gas to produce electricity, and petroleum or diesel for transportation. Hence, CO₂ is of utmost concern compared to other GHGs, and its emission has always been the subject of interest in research discussion about global issues.

Several options can be applied to reduce CO₂ emissions from fossil fuel such as improving the efficiency of fossil fuel combustion, replacing of fossil fuel with renewable one and sequestrating of CO₂ from its large emission sources. Separation and capture of CO₂ from its emission sources are promising options but they remained as great challenges due to some technological and political issues (Mondal *et al.*, 2012). In industrial settings, the separation of CO₂ is an essential step in many industrial processing such as the natural gas purification. The final natural gas used as fuel in the industry or vehicles is consists almost entirely of methane. Removal of CO₂ increases the calorific capacity, yields better transportation conditions and prevents pipeline corrosions. Carbon dioxide content in the natural gas obtained from gas or oil well can vary from 4 to 50% (Datta and Sen, 2006). On the other

hand, purged gas from a gas-reinjected EOR (enhanced oil recovery) well can contain as much as 90% carbon dioxide. Before a natural gas rich in carbon dioxide can be transported, it must be pre-processed so as to meet the typical specification of 2–5% carbon dioxide (Datta and Sen, 2006).

1.2 Conventional technologies for CO₂ separation and capture

Several conventional technologies are available for separation and capture of CO₂ such as; cryogenic distillation, absorption using liquid solvents and pressure-temperature swing adsorption using various solid sorbents. Cryogenic distillation technology has been used for decades for CO₂ removal on the basis of fractional condensation and distillation at low temperature. This technology is a commercial process to produce a large volume of CO₂ with high purity from streams that already have relatively high CO₂ concentrations (>90 %). However, the cost of this technology is very high due to the requirement of extremely low temperature (lower than -73°C for liquefaction of CO₂) and high pressure (Leo *et al.*, 2009; Burt *et al.*, 2009; Olajire, 2010), which leads to high cost.

The absorption process is the commercial technology used for CO₂ separation and capture for more than few decades. Absorption of CO₂ can be either physical or chemical process. In a chemical absorption process, CO₂ is chemically captured from gaseous streams through acid-base neutralization reactions using basic solvents such as monoethanolamine (MEA) to form a weakly bonded intermediate compound. The CO₂-rich solution is pumped to a stripper column for thermal regeneration where the CO₂ is stripped from the solution and the original solvent pumped back for a new cyclic use. The pure CO₂ released from the stripper

is compressed for the subsequent transportation and storage (Yu *et al.*, 2012). High CO₂ recovery rate is about 98% can be achieved with MEA solutions due to fast kinetics and strong chemical reaction (Yang *et al.*, 2008). However, there are many drawbacks of using liquid solvent absorption such as flow problems (flooding and loading) caused by viscosity increases with fast-reacting solvent, equipment corrosion, and high energy consumption for solvent regeneration (Zheng *et al.*, 2005; Gray *et al.*, 2005). For physical absorption process, CO₂ is selectively absorbed in a solvent according to Henry's Law, which means that they are temperature and pressure dependent. Higher CO₂ partial pressure and lower temperature favor the solubility of CO₂ in the solvents. Different physical solvents for CO₂ absorption are commercially available such as dimethylether of polyethylene glycol (Selexol process), propylene carbonate (FLUOR process), cold methanol (Rectisol process) and ionic liquid. Lower energy is required for solvents regeneration due to the weakly interacting between CO₂ and the solvent compared to that of chemical solvents. However, physical absorption has drawbacks due to high capital cost of constructing Selexol and FLUOR plants. In addition, the high viscosity of ionic liquid limits the mass transfer and hence low absorption rates (Olajire, 2010; Yu *et al.*, 2012).

Adsorption is another well-established technology for CO₂ separation and capture. Various regenerable solid sorbents are often used such as activated carbons, metal oxide, hydrotalcite, zeolites, mesoporous silica functionalized with amines and activated alumina. CO₂ molecules are attracted and trapped by the solid sorbents through physisorptions (van der Waals) or chemisorptions (covalent bonding), followed by regeneration (desorption) of the solid sorbents which can be achieved

either by increasing the temperature (Temperature Swing Adsorption, or TSA), or by reducing pressure (Pressure-Swing Adsorption, or PSA) (Olajire, 2010). Physical adsorbents based on carbons and zeolites can adsorb large amounts of CO₂ at room temperature (Hao *et al.*, 2013; Cheung *et al.*, 2013). The rate-limiting step in the adsorption is the diffusion of CO₂ from gas mixture to the inside pore of the adsorbent which is three times higher than the magnitude of CO₂ transfer across the gas-liquid interface in aqueous amine absorption (Khatri *et al.*, 2005). However, these physical adsorbents have many disadvantages due to reduced CO₂ adsorption capacity at high temperature (Zheng *et al.*, 2005; Gray *et al.*, 2005), high temperature requirement for regeneration, poor tolerance to water (Franchi *et al.*, 2005) and unsuitable for high CO₂ concentration streams (> 3%) since it needs frequent regeneration of solid bed.

1.3 Membrane technology for CO₂ separation

Membrane technology is a novel method to facilitate CO₂ separation from a gas mixture. Membranes act as filters that enable continuous separation of one or more gases from a feed mixture based on the differences in physical properties of the gases and/or chemical interplays between the membrane material and the gas (Olajire, 2010). The separation of CO₂ using membrane technologies provides many advantages over the other conventional separation technologies (Zhang *et al.*, 2013). First, the membrane process is a viable energy-saving alternative for CO₂ separation, since it does not require any phase transformation. Second, the necessary process equipment is very simple with no moving parts, compact, relatively easy to operate and control, and also easy to scale-up (Ismail *et al.*, 2009; Zhang *et al.*, 2013). Membrane materials are classified into organic (polymeric) and inorganic (carbon,

zeolite, ceramic or metallic) which can be porous or dense.

There have been several studies of polymeric membranes for gas separation due to its low energy cost, ease in fabrication and scalability (Ismail *et al.*, 2009; Basu *et al.*, 2010). Polymeric membranes can be categorized into two groups; rubbery or glassy; based on operating temperature relative to the glass transition; Rubbery membranes can be operated above the glass transition temperature (Approximate midpoint of the temperature range over which a material undergoes a phase change from brittle to rubbery), while glassy membranes operate below the glass transition temperature (Olajire, 2010; Adewole *et al.*, 2013). However, the loss in permeance stability of polymer membranes at high temperature, high pressure, and highly acidic or alkaline environment has limited its application (Koros and Mahajan, 2000). Furthermore, polymeric membranes show inverse behavior for the permeability/selectivity; in other words, the gas selectivity decreases as the gas permeability through the membrane increases (Zhang *et al.*, 2013). It has been reported that presence of CO₂ even in low concentration induces plasticization problem in polymeric membrane, specially the glassy polymers, due to its condensability at certain pressures. It is supposed that a plasticization phenomenon happens when the polymer matrix absorbs CO₂ present in the feed to an extent that it increases the free volume of the polymer matrix. The swelling of polymer matrix during the absorption of CO₂ enhances the permanent enlargement of interchain spacing in the polymer matrix, which in turn, increases the permeability of gas and decreases the separation performance (Pandey *et al.*, 2002; Baker, 2002; Basu *et al.*, 2010).

Inorganic membranes are gaining intense research efforts for use in CO₂ separation that are difficult to achieve by polymeric membranes with respect to their higher thermal, chemical and mechanical stability (Yeo *et al.*, 2012). Inorganic membranes can be categorized based on their physical structures; either dense or porous. Dense inorganic membranes such as palladium and perovskite are usually used in selective separation of hydrogen and oxygen, respectively (Schiestel *et al.*, 2005; Burkhanov *et al.*, 2011). Porous inorganic membranes are generally consist of a porous thin top layer supported on a porous metal or ceramic support which provides mechanical strength to the system and offers minimum mass-transfer resistance. Porous inorganic membranes that are mainly used include alumina, titania, zirconia, hydrotalcite, silicon carbide, glass, amorphous silica, carbon and zeolites (De Vos and Verweij, 1998; Shekhawat *et al.*, 2003; Kim *et al.*, 2009b; Yeo *et al.*, 2012). These membranes vary in properties such as pore size, surface area, thermal and chemical stability. The porous inorganic membrane can be categorized based on their pore size into microporous (pore diameter <2 nm), mesoporous (2 nm > pore diameter <50 nm) and macroporous (pore diameter >50 nm) (Shekhawat *et al.*, 2003). The microporous inorganic membranes consists essentially of either amorphous silica, carbon molecular sieve or zeolites (Yeo *et al.*, 2012).

Carbon molecular sieve (CMS) membranes are typically prepared through carbonization (at high temperature in an inert atmosphere) of polymeric precursors already processed in the form of membranes (Sim *et al.*, 2013). In spite of higher production cost of CMS membranes which is greater than polymeric membranes by 1 to 3 orders of magnitude per unit area, they provide higher permeance and separation factor compare to polymeric membranes. However, the major

disadvantage of CMS membranes that hinder their commercialization is their brittleness (Brunetti *et al.*, 2010). The zeolite materials are aluminosilicates with uniform pore structures. Zeolite membranes are usually prepared by in-situ hydrothermal synthesis on porous stainless steel, α -alumina, or γ -alumina support tubes or disks for the gas permeation studies (Yang *et al.*, 2008). Despite the success of zeolite membranes in the separation of CO₂ from different gaseous systems, they have two main disadvantages: Firstly, high cost and difficult to produce; Secondly, low gas permeability compared to other inorganic membranes. This is due to the fact that relatively thick zeolite layers are necessary to get a pinhole-free and crack-free zeolite layer (De Beer, 2000).

Mixed matrix membranes (MMMs) are a well-known solution to improve the thermal and mechanical properties of polymeric membranes. MMMS are formed by homogenous incorporation of an inorganic material in the form of micro- or nanoparticles (discrete phase) into a polymeric matrix (continuous phase). The combination of the two different materials provides high selectivity of inorganic phase and low cost of polymer phase that give better design for CO₂-selective membrane. However, the performance of MMMs suffers from defects caused by poor interaction at the molecular sieves/polymer interface which forms non-selective void spaces. Additionally, MMMs encounter plasticization problem caused by CO₂ adsorption (Yang *et al.*, 2008; Ismail *et al.*, 2009; Brunetti *et al.*, 2010).

1.4 Hydrotalcite compound for CO₂ separation

Hydrotalcite (HT) is a class of anionic clays called layered double hydroxide (LDH) or hydrotalcite-like compounds. The general chemical formula of hydrotalcite

is $[M_{1-x}^{2+}M_x^{3+}(\text{OH})_2](\text{A}^{n-})_{x/n} \cdot m\text{H}_2\text{O}$, where M^{2+} the divalent cation (e.g., Mg^{2+} , Ni^{2+} , Co^{2+} , Zn^{2+} , Cu^{2+}); M^{3+} is the trivalent cation (e.g., Al^{3+} , Fe^{3+} , Cr^{3+}); A^{n-} is the anion (e.g., CO_3^{2-} , SO_4^{2-} , NO_3^- , Cl^-) and x is the ratio of $(M^{3+}/M^{2+} + M^{3+})$ with values range from 0.2 to 0.33. These materials exist with positively charged layers of brucite $[\text{Mg}(\text{OH})_2]$, and aluminum hydroxide $[\text{Al}(\text{OH})_3]$, which are balanced by anions and water molecules in the interlayer region as shown in Figure 1.1 (Reichle, 1985; Cavani *et al.*, 1991; Salomão *et al.*, 2011). HT compounds have attracted much attention worldwide since they find a wide range of applications. Various important applications include catalysis in dehydrochlorination and recovery of hydrochloric acid (Kameda *et al.*, 2007) and decomposition of urea (Vial *et al.*, 2006). HT has already found use in pharmaceutical industries as a drug carrier (Lee and Chen, 2006). HT can also be applied in the purification of wastewater as sorbent to remove phosphates or heavy metals (Li *et al.*, 2009). In particular, HT has been intensively investigated in recent years as adsorbents for CO_2 at high temperature to reduce the greenhouse emission into atmosphere. HT has adequate mechanical strength when it is exposed to high pressure, it exhibits high capacity and selectivity to adsorb CO_2 at high temperature, adequate CO_2 adsorption/desorption kinetics for CO_2 at operating conditions, and stable adsorption capacity of CO_2 after repeated adsorption/desorption cycles (Yong *et al.*, 2002). The CO_2 adsorption capacity of HT is influenced by many factors such as aluminum content, anion type, water content as well as the heat treatment temperature. The effect of these factors on CO_2 adsorption at high temperatures was investigated on several commercially supplied HTs at higher temperatures (300 °C). Their results revealed that the capacity for CO_2 increases when the amount of aluminum was decreased and that there is an optimum aluminum content in the HTs for adsorption of CO_2 . The presence of small amount of

water in the HTs also favors the adsorption capacity. Similarly, under dry and wet feed condition, the capacity for the wet feed conditions was found to be approximately 10% higher than for the dry feed condition. Adsorption capacities of HTs having CO_3^{2-} and OH^- anion reveal that the HTs containing CO_3^{2-} show higher adsorption capacities than those containing OH^- (Baba *et al.*, 2010). However, researches on the fabrication of HT material as a CO_2 selective membrane has been rarely conducted (Othman, 2009; Kim *et al.*, 2009a).

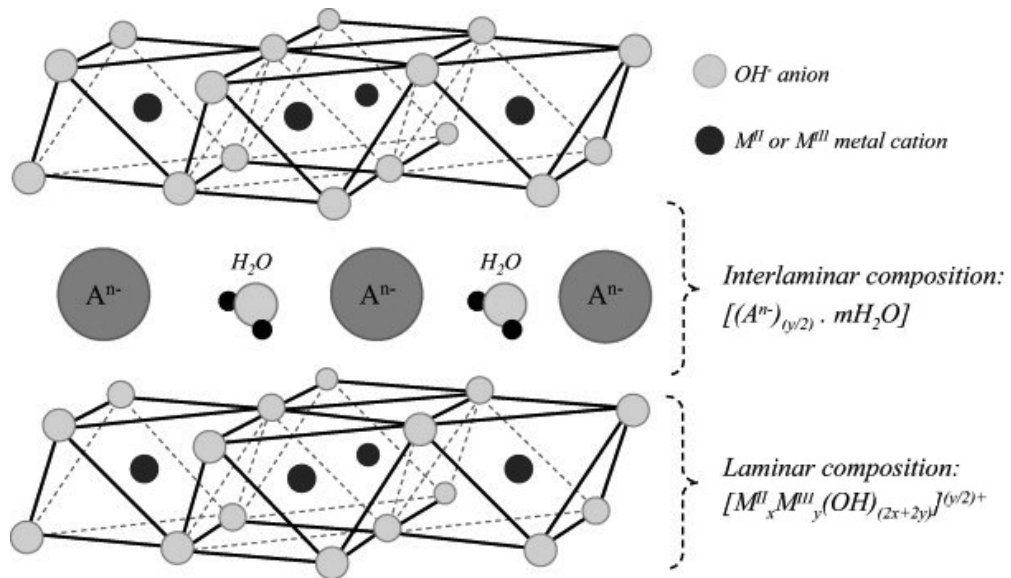


Figure 1.1: Schematic representation of the HT structure (Salomão *et al.*, 2011)

1.5 Problem statement

The inorganic membrane has been widely studied for preparation and modification of CO_2 -selective membranes because of its high resistance against heat and chemicals (Yeo *et al.*, 2012). However, the attempt to prepare uniform and thin inorganic membrane is a very challenging work. Many factors affect the production of high quality inorganic membrane. These include: the right choice of synthesis method and suitability of preparation conditions. The most important features of the

good CO₂-selective membrane are high CO₂ permeation flux and selectivity for CO₂ from the gaseous mixture. High CO₂ permeation flux reduces the required membrane area and high CO₂ separation selectivity under low driving force is important to confirm the high separation efficiency of the prepared membrane, therefore the capital separation cost will be reduced (Lu *et al.*, 2007). However, the membrane performances have to balance between CO₂ permeation flux and CO₂ separation selectivity. Generally, the increasing membrane thickness decreases the gas permeation flux, but at the same time increases the gas separation selectivity. The synthesis of a defect free and thin membrane layer is desirable for both high gas separation selectivity and gas permeation flux. This is one of critical issue along with the challenges to prepare a membrane with the desired characteristics.

The inorganic molecular sieve membranes made from zeolite, carbon and silica currently suffer problems such as brittleness and low permeability. In this work, a molecular sieve hydrotalcite membrane is prepared and characterized for the first time in order to investigate its potential to solve some of the issues faced by the membranes described earlier. Its separation performance with the other molecular sieve membrane namely pure silica membrane is also compared. Hydrotalcites are very attractive materials for CO₂ adsorption at elevated temperature in the presence of water. Therefore, in this research the fabrication of new membrane from HT material modified porous alumina and silica membranes to increase the separation selectivity of CO₂ from different gaseous mixtures is a subject of this study. Modification of the internal pore surface of alumina membrane with HT increases the amount of adsorbed CO₂ resulting in increase of the CO₂ diffusion and separation selectivity. The composite membrane of HT-alumina is expected to

provide high gas permeation flux due to the bigger pore size of alumina (mesoporous) and adequate separation factor.

Separation of gas using membranes follows a few mechanisms. In molecular sieve mechanism, the separation is based on the kinetic diameter of the gas molecules. The gas with small kinetic diameter penetrates through the pores, whereas the larger kinetic diameter cannot pass through these pores. High gas selectivity and permeation flux for the small gas molecules in a gas mixture can be achieved from molecular sieve membranes. However, the separation selectivity and gas permeation flux can further improve the interaction between gas molecules and pore wall, resulting in an additional transport along the surface. The second mechanism called surface affinity for porous materials can also drastically decrease or eliminate the transport of weakly adsorbed molecules through the pore by reducing the size of pore mouth by the adsorbed molecules (Moon *et al.*, 2004). Separation layers can be chemically modified in order to change the surface affinity of the membranes. In this way the pore size can be changed and/or the chemical character of the surface can be modified (Keizer *et al.*, 1988). With smaller pore size it is expected that the gas-solid interaction and surface affinity play a bigger role than the other gas diffusion phenomena.

1.6 Research objectives

This research is aimed at developing a novel porous HT membranes with molecular sieve characteristics for CO₂ separation from natural gas, flue gas and fuel streams. The present research study has the following objectives:

1. To develop and synthesize HT-modified porous membranes by sol-gel method at different HT vol. % and sintering temperature.
2. To characterize and analyze the physical and chemical properties of HT-modified porous membrane.
3. To evaluate and study the performance of HT-modified porous membranes for single gas CO₂, H₂, N₂, and CH₄ permeances and permselectivities over wide range of pressure differences and operating temperatures.
4. To study the performance of HT-modified porous membrane for CO₂ permeation and separation from different binary gaseous mixtures contains CO₂/CH₄, CO₂/N₂ and CO₂/H₂ over different range of operating parameters (operating temperature, pressure difference across the membrane and CO₂ feed concentration).
5. To optimize and build up an empirical model for CO₂ permeance and CO₂ separation selectivity for different mixed gas mixtures contains CO₂/CH₄, CO₂/N₂ and CO₂/H₂.

1.7 Research scope

This research focuses on the synthesis, development and characterization of porous membranes modified with HT as a CO₂ affinity membrane. For this purpose, different HT vol. % in the composite membrane and different sintering temperatures are to be investigated carefully. The synthesized membranes are characterized in order to understand its chemical structure, surface morphology, CO₂ adsorption capacity, porosity and pore size distribution. The steps outlined below leads to the accomplishment of the research objectives. These are:

1.7.1 Synthesis of unmodified alumina and silica membranes via sol-gel method

The alumina membrane is synthesized from sol-gel method following the documented work in (Ahmad *et al.*, 2005; Ahmad *et al.*, 2006b). In this research 2 vol.% of PVA solution containing 4 g of PVA in 100 mL of water is used as a binder, as reported previously that this ratio of binder is adequate to achieve an appropriate porosity level to avoid cracks on the gel layer. Whereas, the silica membrane is synthesized from sol-gel method following the procedures reported by (De Vos and Verweij, 1998; Peters *et al.*, 2005). The polymeric silica sol was prepared by hydrolysis and condensation of tetraethylorthosilicate (TEOS) in ethanol with nitric acid (HNO₃) as catalyst. The standard molar ratios of TEOS-ethanol-water-HNO₃ are used.

1.7.2 Development of alumina and silica membranes with HT material via sol-gel method

HT sol was prepared from sol-gel technique by controlling hydrolysis and condensation of aluminum tri-sec butoxide and magnesium methoxide following the documented work (Valente *et al.*, 2007; Prince *et al.*, 2009). The HT-alumina membrane was prepared by mixing together the freshly prepared alumina sol with HT sol at different volume ratio followed by dip coating the support in this mixed sol. Whereas, the HT-silica membrane was prepared by mixing together the freshly prepared silica sol with HT sol at different volume ratio followed by dip coating the support in this mixed sol and sintering it at different temperature.

1.7.3 Characterization of unmodified and the modified porous membranes

The synthesis membrane samples will be characterized and re-evaluated using the following equipment:

- X-ray diffraction (XRD) technique will be used to characterize the membrane internal structures and compositions of the membrane. The XRD patterns should suggest the presence of HT in the porous membrane sample.
- Fourier Transform Infrared spectrometry (FTIR) test will be used for the determination of surface functional groups. These functional groups govern the activity of the membrane.
- Brunauer-Emmett-Teller method (BET) method will be used to determine the surface area, pore size, volume and pore size distribution for the suggested membrane. These physical properties of the membrane govern the permeability and selectivity of the membrane because they indicate whether that the CO₂ gases can penetrate through the membrane pore or not. That permeability determines the amount of CO₂ that can permeate through the membrane and the separation factor from other gases.
- Thermo gravimetric analyzer (TGA) technique will be used to determine the changes in membrane weight in relation to the change in temperature. Also, TGA analysis will be used to determine the CO₂ adsorption and desorption of the adsorbent through the change membrane in membrane weight when CO₂ gas is fed instead of N₂.
- Since it is of importance to characterize the surface topography and morphology of the membranes, scanning electron microscopy (SEM) will be employed for this purpose.

1.7.4 Study of the permeation of single gas and mixed gas mixtures using modified HT porous membrane

All the unmodified and modified membranes with HT are subjected to preliminary single gas permeations of CO₂, H₂, N₂ and CH₄ at 30 °C and 100 kPa. The modified HT membrane that has highest permselectivity performances of CO₂/CH₄, CO₂/N₂ and CO₂/H₂ will be selected for single gas and mixed gas permeation studies over operating temperature range 30-190 °C and pressure difference across the membrane of 100-500 kPa. In the mixed gas permeation and separation studies, three binary gas mixture were carried out CO₂/CH₄, CO₂/N₂ and CO₂/H₂ using the selected modified membrane over operating temperature of 30-190 °C and pressure difference across the membrane of 100-500 kPa and CO₂ feed concentration of 10-50%.

1.7.5 Modeling, optimization for CO₂ permeance and separation selectivity from mixed gas mixture and surface affinity study

Design of experiments (DoE) was chosen to optimize and find out empirical equations for CO₂ permeances and separation selectivities of the three binary gas systems of CO₂/CH₄, CO₂/N₂ and CO₂/H₂ using Design Expert software version 6.0.6. The optimization of the process parameters was determined by using response surface methodology (RSM) coupled with center composite design (CCD). Whereas the statistical model equations are determined using quantitative data from the set of experimental runs.

1.8 Organization of thesis

The thesis consists of five chapters and each chapter gives specific information about this research project.

Chapter 1 (Introduction) presents a brief introductory of this research project. This chapter starts with the global issues and the importance of the CO₂ separation. This chapter also gives brief overview of the conventional and membrane technologies for CO₂ separation and the definition of HT compound and its application in CO₂ separation. At the end of this chapter, problem statements that provide basis and rationale to justify the research direction in the present study are elaborated. Based on the problem statement; the specific objectives of the research followed by the research scope are stated clearly in this chapter.

Chapter 2 (Literature review) presents literature review on the background of the present research project. This chapter provides the literature review on the modification of γ -alumina membrane for CO₂ separation, in addition to the sol-gel method for synthesis of γ -alumina membrane. The methods used for synthesis and modification of silica membrane for CO₂ gas separation are also provided. Further in this chapter are reviews on the hydrotalcite compound for CO₂ adsorption, the sol-gel method used for preparation of hydrotalcite and the efforts on fabrication of hydrotalcite membrane. At the end of this chapter, the gas transport mechanisms through inorganic porous membrane are discussed.

Chapter 3 (Materials and Methods) describes the detail of materials and methodology used in this research project. The first part of this chapter presents the

list of all materials and chemicals used in present research project. The subsequent topics describe clearly the experimental procedures for synthesis method of membrane support, unmodified alumina and silica membranes, modified alumina and silica membranes with HT, characterization methods and analytical techniques. At the end of this chapter, details of experimental procedures of the gas permeation and separation test in measuring the gas permeation and separation and also gas sample analysis are elaborated.

Chapter 4 (Results and Discussion) presents the experimental results and discussion of the present research project. The first section of this chapter presents the characterizations of unmodified and modified porous membranes with HT. The subsequent topic presents the preliminary single gas permeations comparison between the synthesized membranes. This is followed by single gas permeation of CO₂, H₂, N₂ and CH₄ and mixed gas permeation and separation studies of three systems CO₂/CH₄, CO₂/N₂ and CO₂/H₂ through the selected modified membrane with HT. In the last part of this chapter, DoE approach was discussed to optimize the operating parameters and build up empirical equations to represent CO₂ permeances and separation selectivity for the three systems of CO₂/CH₄, CO₂/N₂ and CO₂/H₂.

Chapter 5 (Conclusions and Recommendations) gives the conclusive attainment of all the major finding obtained in this research project. Suggestions and recommendations for future work to improve the present research work are also presented.

CHAPTER 2

LITERATURE REVIEW

This chapter provides the literature review of application of γ -alumina in gas separation, the methods used to enhance the surface diffusion and the synthesis fundamentals of γ -alumina membrane by sol-gel method. Next, various methods used in the synthesis of silica membrane for gas application are reviewed. The following section also reviews the modifications of silica membrane by doping elements to enhance its properties. Further in this chapter are reviews on the synthesis methods of hydrotalcite compounds and the synthesis of hydrotalcite membrane. Finally, literature review on the gas transport mechanisms for inorganic membranes is also provided.

2.1 γ -alumina membranes for gas separation

Although the synthesis of mesoporous γ -alumina membranes stalled in the early 1980's, many valuable experimental details were revealed. These details included type of metal-organic compound, temperature of hydrolysis, amount and type of acid used as a peptizing agent, amount of binder adding to create defect free membrane and permeability of gases (Leenaars *et al.*, 1984; Leenaars and Burggraaf, 1985b; Leenaars and Burggraaf, 1985a; Othman *et al.*, 2001; Kwon *et al.*, 2012). Inorganic mesoporous alumina material have been selected to prepare a membrane for CO₂ gas separation since it is thermally and chemically stable and has good mechanical strength (Kwon *et al.*, 2012). Generally, the mesoporous alumina membrane provides high gas permeance but low selectivity due to transport of the gases through the pores by Knudsen diffusion mechanism in which the light gases

permeate faster than heavy gases (Mukhtar and Othman, 2004). A well-known example is Knudsen separation of uranium isotopes (Keizer *et al.*, 1988). Higher Knudsen separation values are obtained for light gases such as H₂/CO₂ with a separation factor of 4.7. Moreover, mesoporous γ -alumina membranes had an essential function as intermediate layer on macroporous supports in order to provide a smooth pore size transition between the support and the more selective microporous silica membranes (Xomeritakis *et al.*, 2009). Therefore, to achieve high separation factors, different mechanisms for gas transport through γ -alumina have to be employed.

Separation factors can be enhanced by introducing an interaction between one of the gases in the mixture and the membrane pore surface. If the adsorbed gas is mobile along the surface of the pore wall, it will diffuse in the direction of decreasing driving forces. The additional diffusion enhanced the gas permeance and separation factor of the more adsorbed gas. The presence of this type of transport, called surface diffusion, is frequently described in porous materials (Othman, 2009).

A few efforts have been reported to improve γ -alumina membranes to facilitate CO₂ surface diffusion. Keirzer *et al.* (1988) and Uhlhorn *et al.* (1989b) modified the γ -alumina membrane with magnesia (MgO) by impregnating technique to improve CO₂ surface diffusion and conform an increase in CO₂ adsorption. However, the modified membrane showed CO₂/N₂ separation factor of only unit nearly to the Knudsen separation factor value, 0.8. They suppose that strong adsorption of CO₂ occurred on the MgO sites, resulting in a decrease in CO₂ permeation rate.

Cho et al. (1995) improved the CO₂ surface diffusion by doping calcium oxide (CaO) into the γ -alumina membrane. The CO₂/N₂ separation factor was enhanced to be 1.72 at 25 °C and decreased with increase in the temperature to reach 1.5 at 200 °C. It was concluded that the separation factor could be enhanced by applying surface diffusion mechanism when the membrane is microporous and the operating temperature is low.

Hyun et al. (1996) modified the top layer of γ -alumina composite membranes supported on α -alumina and titania by silane coupling with phenyltriethoxysilane to improve the CO₂ affinity. It was found that the separation factor of the modified γ -alumina membranes with silane coupling was strongly dependent on the hydroxylation tendency of the support materials and the amount of phenol radical. The CO₂/N₂ separation factor through the γ -alumina-titania membrane modified with the 10 wt. % silane solution was 1.7 at 90 °C and pressure difference of 200 kPa for the equimolar binary gas mixture, whereas, there was no improvement of CO₂/N₂ separation factors in the α -alumina supported case.

Lee et al. (2005) and (2006) investigated the effect of adsorption capacities of different gas species He, N₂, CH₄, C₂H₆ and CO₂ on the permeation properties of mesoporous γ -alumina supported on α -alumina. It was observed that the permeation of the adsorbing gas species (C₂H₆ and CO₂) increased through preferential adsorption on the membrane pore surface. It was observed that the permeance of the adsorbing gas components (C₂H₆ and CO₂) in the single gas system increased through preferential adsorption on the membrane pore surface more than the predicted value by the Knudsen diffusion. While for binary gas systems, the

adsorbing gas component limited the diffusion of the weakly adsorbing gas through the γ -alumina membrane. It was concluded that the improvement in the adsorption capacity of membrane could enhance the separation factor in the presence of the adsorbing gas component due to the surface diffusion mechanism.

2.1.1 Synthesis of γ -alumina membrane by sol-gel method

The sol-gel process is the most practical method for fabrication of micro or meso porous inorganic membranes. The process involves the transition of suspension colloidal particles in a liquid system called sol into a semi-rigid solid network linked together by surface forces called gel. Therefore the term “sol-gel” processing can be used to describe wet chemical synthesis of inorganic materials in which eventually a particulate gel is produced. The sol-gel process starting from transformation of inorganic molecular precursor (metal alkoxide) into a highly cross linked solid (inorganic polymer) by hydrolysis and condensation reactions. Metal alkoxides have the general formula $M(OR)_z$ where M is a metal of valence z and R is an alkyl group (Rahaman, 1995). Alumina alkoxides $Al(OR)_3$ where $R = (C_4H_9)$ are commonly used as a metal precursor for synthesis of alumina membrane from sol-gel method due to easily hydrolyzed by water to form hydroxides. The hydrolysis step replaces an alkoxide with a hydroxide group from water and a free alcohol (butanol) is formed as follows:



Once hydrolysis has occurred the sol can react further and condensation (polymerization) occurs resulting in boehmite ($AlOOH$) sol.



The following reaction might also be possible, provided that the coordination number of alumina was satisfied to cause the nucleophilic attack which initiated and facilitated water condensation reaction, giving rise to the production of alumina after liberation of water (Teoh *et al.*, 2007; Othman and Kim, 2008b).



During hydrolysis step hydrochloric or nitric acid can be added into the boehmite mixture to facilitate peptization of the solution to a clear sol so that highly dispersed metals in the solution can be obtained (Yoldas, 1975; Othman *et al.*, 2001). Changrong *et al.* (1996) investigated the effect of acidity on the boehmite sol properties. Stable boehmite sol was prepared by hydrolysis of aluminum tri-sec butoxide in hot distilled water at temperature above 80 °C and nitric acid was used as a sol peptizer. It was found that the size and shape of the sol particles as well as the viscosity affected by its acidity. For low acidity the sol particles was needle or rod shaped with diameters of a few nanometers and length around a hundred nanometers. Whereas, the sol particles change to granular or spherical shaped with diameter of 10-20 nm at high acidity conditions. On the other hand, the sol viscosity increased sharply with increase the acidity resulted in more chain between the particles and finally a tendency for gelation at high acidic conditions. The optimum mole ratio of acid to alkoxide used to obtain stable boehmite sol useful for synthesis crack free alumina membranes was around 0.07 (Ahmad *et al.*, 2008; Kwon *et al.*, 2012).

The crack formation during gels drying is the biggest challenge in the synthesis of γ -Al₂O₃ membrane from sol-gel process. Normally, organic binders are

added to the boehmite sol to avoid cracking formation in the initial drying process and during heat treatment. Polyvinyl alcohol (PVA) and polyethylene glycol (PEG) were found to be the most effective binders in the preparation of crack free γ -Al₂O₃ membrane (Lambert and Gonzalez, 1999; Othman *et al.*, 2001; Ahmad *et al.*, 2008). Othman *et al.* (2001) investigated the effect of PVA content on the characteristics of the sintered γ -Al₂O₃ membrane. It was demonstrated that the increase in PVA addition caused essential increase in the boehmite sol viscosity. High-viscosity sols form γ -Al₂O₃ membranes developed cracks during drying and sintering. On the other hand, the pore size of the sintered membrane increased with the increased PVA content. It was concluded that defect free γ -Al₂O₃ membrane with small pore size was prepared using 2 vol. % of PVA solution containing 4 g PVA in 100 ml of water.

Mesoporous γ -Al₂O₃ membranes were prepared by dip coating of boehmite sol onto α -alumina support and drying at room temperature for 24 h (Othman *et al.*, 2001; Ahmad *et al.*, 2006b). The dried membranes were then sintered to get the final membrane. The membrane thickness was found to depend on the sol viscosity, dipping time and on the support pore size (Leenaars *et al.*, 1984; Othman *et al.*, 2001). However, multiply coating of the γ -Al₂O₃ membrane on the support was applied to avoid crack formation.

2.2 Silica membranes for gas separation

Silica is considered an interesting material in the fabrication of CO₂ selective membranes due to its low cost, availability and unique properties. It shows exceptional thermal, chemical, and structural stability in both oxidizing and reducing